US and CT Evaluation of Acute Pelvic Pain of Gynecologic Origin in Nonpregnant Premenopausal Patients[1]

Andrew W. Potter, MD • Chitra A. Chandrasekhar, MBBS

ONLINE-ONLY CME

See www.rsna.org/education/rg_cme.html

LEARNING OBJECTIVES

After reading this article and taking the test, the reader will be able to:

- Discuss the normal physiologic processes that may lead to the development of acutely painful pelvic lesions in women.
- Describe the US and CT characteristics of the most common causes of acute pelvic pain in women.
- Correlate the US and CT imaging appearances of acutely painful pathologic conditions in the female pelvis.

TEACHING POINTS

See last page

The interpretation of imaging findings in the premenopausal patient with acute pelvic pain is influenced by knowledge of the physiologic changes that occur in the pelvis as well as by the patient's clinical history. Although ultrasonography (US) is the modality of choice for initial imaging, gynecologic disease is detected or suspected with increasing frequency at computed tomography (CT) because of the increasing availability and use of this modality. As a result, the recognition of common features of gynecologic entities on both US and CT images is essential for prompt diagnosis and expeditious management. Categorizing lesions according to their anatomic location, physiologic or pathologic origin, and internal characteristics (cystic, solid, or mixed) allows efficient and accurate diagnosis.

RadioGraphics 2008; 28:1645–1659 • **Published online** 10.1148/rg.286085504 • **Content Codes:** CT ER OB US

[1]From the Department of Diagnostic and Interventional Radiology, University of Texas Health Science Center at Houston, 5656 Kelley St, Houston, TX 77026. Presented as an education exhibit at the 2007 RSNA Annual Meeting. Received January 30, 2008; revision requested March 14 and received April 1; accepted April 7. All authors have no financial relationships to disclose. **Address correspondence to** A.W.P. (e-mail: *Andrew.W.Potter@uth.tmc.edu*).

Introduction

Acute pain of pelvic origin is a common symptom necessitating emergent medical evaluation. The duration of acute pelvic pain may range from several hours to several days, and its possible causes span a gamut from functional ovarian cysts that require routine follow-up to adnexal torsion and ectopic pregnancy requiring urgent surgical management. All these events occur in premenopausal patients, and prompt diagnosis allows potentially ovary-sparing or life-saving surgery (1).

Clinical evaluation and laboratory testing are essential when a gynecologic condition is suspected to be the cause of acute pelvic pain. For the initial diagnostic imaging evaluation, ultrasonography (US) is the modality of choice. High-frequency endovaginal transducers allow excellent anatomic depiction and pathologic characterization. However, computed tomography (CT) also is often performed in patients with referred pain beyond the pelvis or in those who present after hours. The general after-hours availability of CT scanners contributes to the increasing frequency of the use of CT to evaluate patients with acute pelvic pain. As a result, knowledge of both the US and the CT features of acutely painful gynecologic conditions is beneficial.

Given the many possible causes of pelvic pain, a structured approach to image interpretation is necessary to narrow the differential diagnosis. First, the distinction between pregnant and nonpregnant patients, as determined by beta human chorionic gonadotropin (β-hCG) levels in correlation with menstrual history, is crucial. This clinical information portends the physiologic changes that may be expected and allows accurate image interpretation.

Pathologic gynecologic conditions may be grouped, first, according to their anatomic origin. Further, US and CT characterization of lesions as simple cysts, complex cysts, or mixed cystic or solid structures helps narrow the diagnostic possibilities. It is important also to remember the general difficulty of distinguishing between lower abdominal pain and pelvic pain. Pelvic pain may exist in the absence of a gynecologic cause, and US and CT images may depict nongynecologic disease if the initial imaging protocols are not tailored too narrowly within the pelvic region (2).

Ovaries

Ovarian cysts are a common source of acute pelvic pain. Many ovarian cysts are physiologic in origin. Normal physiology drives the monthly emergence of one or more dominant follicles. Pelvic pain may occur as the follicle matures and the ovarian capsule is stretched, at the time of ovulation (*Mittelschmerz*), or after cyst rupture or hemorrhage. Any mass ovarian lesion predisposes the ovary to torsion on its vascular pedicle, although torsion also occurs in the absence of an ovarian mass in prepubertal girls.

Follicular Cysts

Ovarian follicles are estrogen sensitive. Most remain nonovulatory, have a diameter of less than 10 mm, and are routinely depicted at US and CT (Fig 1). The persistent absence of nonovulatory follicles is suggestive of a peri- or postmenopausal state. During the first half of the menstrual cycle, follicle-stimulating hormone drives follicular enlargement at a rate of roughly 2 mm per day. Eventually, one or more dominant (Graafian) follicles with a diameter of 18–25 mm emerge. (Although these enlarged follicles are cystic in nature, it is appropriate to refer to them as follicles and reserve the term *cyst* for structures larger than 2.5–3.0 cm.) A surge in luteinizing hormone then triggers ovulation and the conversion of the dominant follicle into the corpus luteum (3).

When a dominant follicle fails to expel an oocyte, the follicle may further enlarge into a cyst. Follicular cysts often measure 3–8 cm in diameter and may remain hormonally sensitive. In pregnancy (with successful ovulation from another follicle), placental gonadotropin production causes luteinization of the follicular cyst, which may enlarge to as much as 25 cm. Most cysts are asymptomatic and incidentally discovered, if they are discovered at all. However, pain may develop because of rapid cystic enlargement, rupture, or hemorrhage, alone or in combination.

Follicular cysts are the most common well-defined adnexal masses. Arising from and compressing the adjacent ovarian parenchyma, they are easily recognized and localized at US and CT. At US, a lesion may be identified as intraovarian if it is surrounded by a rim of follicle-containing ovarian tissue. Follicular cysts are unilocular, contain anechoic fluid, and produce posterior through-transmission of sound waves (Fig 2a). Minimal low-level echoes related to proteina-

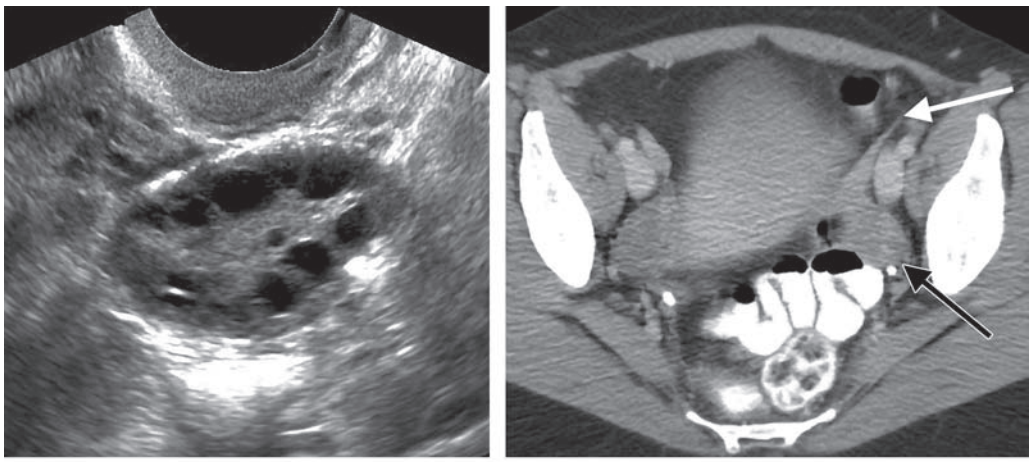

a. b.

Figure 1. Normal ovarian follicles. **(a)** Longitudinal transvaginal US image of the ovary reveals peripherally located nonovulatory follicles that might be mistaken for cysts. **(b)** Axial contrast-enhanced CT image shows the low attenuation typical of the normal ovary (black arrow), with a faintly depicted follicular structure. Location of the ovary close to the external iliac vessels and posterior to the round ligament (white arrow) aids in its identification.

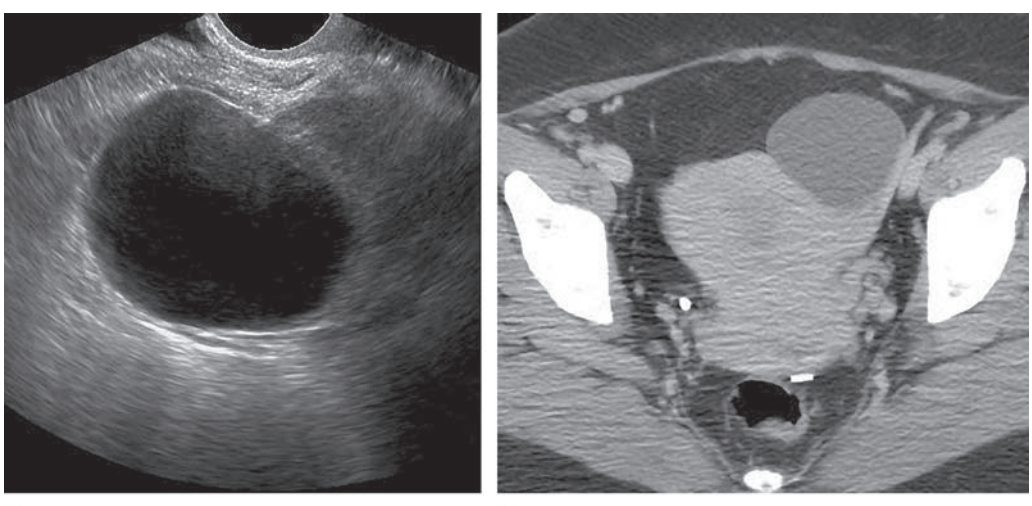

a. b.

Figure 2. Simple left ovarian cyst. Transverse transvaginal US image **(a)** and axial contrast-enhanced CT image **(b)** show a well-defined adnexal fluid collection that is anechoic and hypoattenuating.

ceous fluid or cellular debris may be present and are always mobile. Cysts that are discovered incidentally typically involute and resolve in the course of one to two menstrual cycles. Follow-up US to verify their resolution is best performed on days 5–10 (follicular phase) of a subsequent menstrual cycle. Large follicular cysts may persist beyond a single menstrual cycle, and, less commonly, may endure through several cycles. There may be some overlap in appearance between follicular cysts and cystadenomas; however, the latter tend to be larger and more persistent, and they are more often found in older women.

At CT, a follicular cyst appears as a well-defined round simple fluid collection with thin nonenhancing walls (Fig 2b) and with internal attenuation

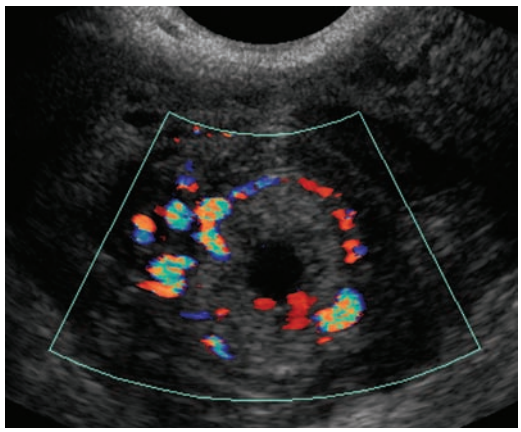

Figure 3. Corpus luteum. Transverse transvaginal color Doppler US image depicts the thick walls and increased peripheral vascularity of a newly formed corpus luteum.

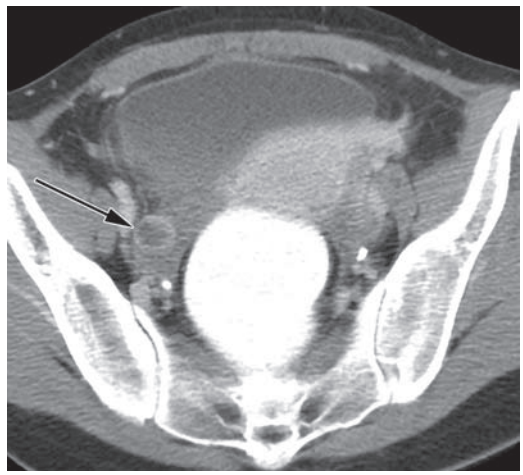

Figure 4. Corpus luteum cyst. Axial contrast-enhanced CT image demonstrates enhancement of the wall of a right corpus luteum (arrow) with a small amount of adjacent free fluid, a finding suggestive of a ruptured luteal cyst.

that is generally less than 15 HU. When a follicular cyst is incidentally detected at CT, US need not be performed immediately for confirmation and may be deferred until the routine follow-up evaluation (4).

Cystic Corpus Luteum

When ovulation and implantation have occurred, luteinizing hormone drives the transformation of the remaining follicular bed into the corpus luteum. The granulosa cells of the follicle, previously avascular, undergo marked neoangiogenesis. The newly developed vasculature allows the delivery of progesterone produced by the corpus luteum into the maternal circulation but also predisposes the corpus luteum to hemorrhage. The corpus luteum is maintained by circulating β-hCG, which has an effect similar to that of luteinizing hormone. The corpus luteum normally regresses at the end of the first trimester, as the placenta becomes the dominant source of progesterone. Either the failure of the corpus luteum to involute or its hemorrhage may result in cystic enlargement. The distinction between a hemorrhagic corpus luteum and a corpus luteum cyst is largely arbitrary, with some authors using a size of 2 cm as the threshold differentiating a cyst (5).

The walls of luteal cysts are thicker than those of follicular cysts on both US and CT images and may be irregular because of a recent rupture or an adherent blood clot. The internal contents of the corpus luteum may be anechoic or isoechoic at US, depending on the degree and age of hemorrhage. Posterior through-transmission helps differentiate the corpus luteum from a solid mass, which may have echogenic components and a posterior shadow (6). Color Doppler US depicts increased peripheral vascularity of the corpus luteum (Fig 3).

Wall enhancement at CT is caused by the proliferation of blood vessels. Luteal cysts are often unilocular, with thick, crenulated walls (7). Attenuation of the luteal cyst is high because of the intracystic presence of blood products. When rupture has occurred, CT depicts fluid surrounding the adnexa (Fig 4).

Hemorrhagic Ovarian Cysts

Hemorrhage into a follicular cyst or corpus luteum generates pain and may lead to an emergent presentation. There is considerable overlap in the imaging appearance of hemorrhagic follicular and corpus luteum cysts, and their differentiation is dependent primarily on the clinical history. Temporal correlation of a symptomatic cyst with the luteal phase of the menstrual cycle or with a positive β-hCG level favors the diagnosis of hemorrhagic corpus luteum.

The US pattern varies according to the age of the hemorrhage and the degree of clot for-

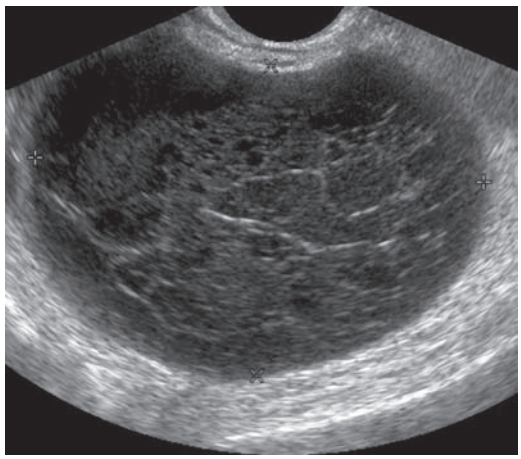

Figure 5. Hemorrhagic ovarian cyst. Transverse transvaginal US image of the adnexa shows a complex hemorrhagic cyst with the characteristic lacelike echogenic pattern of fibrin strands that form as blood clots and retracts.

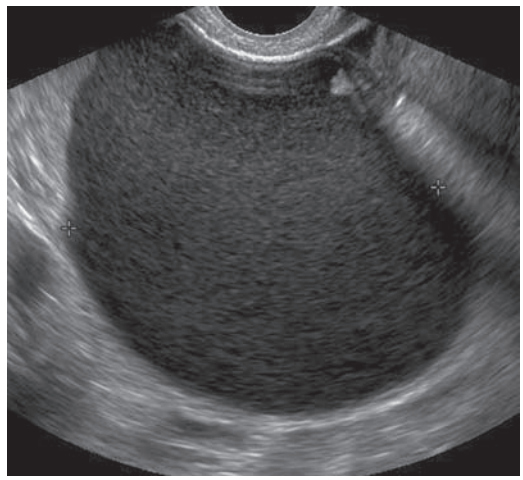

Figure 6. Endometrioma. Longitudinal transvaginal US image of the adnexa depicts a large, well-defined, complex cystic mass with low-level internal echoes.

mation. The typical appearance is that of a complex mass with internal echoes and some degree of posterior through-transmission. Although fresh blood may be anechoic initially, a hemorrhagic cyst is defined by low-level echogenicity in a fine, lacelike, reticular pattern for the first 24 hours, and this pattern is diagnostically specific (6,8) (Fig 5). As clot retraction occurs, US may depict triangular or curvilinear echogenic regions at the cyst wall. Fluid-debris levels develop as the clot liquefies.

Teaching Point

Hemorrhagic ovarian cysts before rupture often appear unilocular on CT images, with an internal attenuation of 25–100 HU. Fluid-fluid levels and hemoperitoneum may be observed after cyst rupture. When hemorrhagic ovarian cysts are detected initially at CT, they need not be immediately evaluated with US unless there is substantial hemoperitoneum. Instead, follow-up US may be performed within one or two menstrual cycles to determine whether the cyst has resolved (7).

Endometriomas

Endometriosis affects an estimated 10% of premenopausal women. Ectopic endometrial tissue is estrogen sensitive, and it proliferates and bleeds synchronously with the endometrium. Without the normal drainage pathway of the vagina, bleeding from endometrial implants in the adnexa, uterosacral ligaments, or peritoneum often causes cyclic pelvic pain. The imaging-based detection of endometriosis is not currently possible because the multiple diffuse implants are too small. As much as 80% of ectopic endometrial tissue is found in the ovaries. When larger focal deposits of endometrial tissue are present in the ovary, these endometriomas are detectable at imaging (9). Secondary rupture or infection of an endometrioma may lead to acute presentation, but such occurrences are uncommon.

Endometriomas are complex cystic masses. A US finding of uniform low-level echogenicity or a ground-glass appearance is a result of repeated episodes of cyclic bleeding and corresponds to the finding of a "chocolate cyst" at gross examination (Fig 6). Large endometriomas may be depicted as multiple adjoining cystic structures; less frequently, they appear solid (10). Endometriomas larger than 3 cm often destroy portions of the ovary as normal ovarian tissue stretches to accommodate the cyst.

Rupture of the endometrioma and the ensuing blood products produce adhesions. Resultant fibrosis creates complex masses that may simulate pelvic inflammatory disease, hemorrhagic cysts, or even malignancies (11). The CT appearance of endometriomas is variable and includes solid and cystic heterogeneous adnexal masses. The margins of the mass may be irregular, with internal regions of low attenuation resulting from cyclical

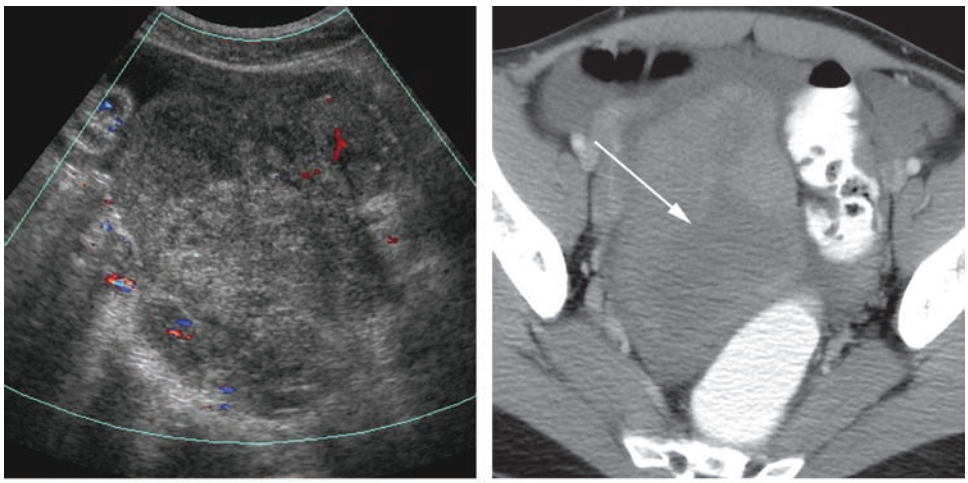

a. b.

Figure 7. Endometrioma with a hemorrhagic component. **(a)** Transverse transabdominal color Doppler US image of the adnexa demonstrates a lobulated mass with a heterogeneous echotexture and minimal internal vascularity. **(b)** Axial contrast-enhanced CT image shows an irregular but well-demarcated right adnexal mass with areas of decreased attenuation (arrow) that represent old hemorrhage.

episodes of bleeding (Fig 7). Both US and CT findings have low specificity for the diagnosis of endometriomas. Follow-up imaging is useful for differentiating endometriomas from pathologic entities such as hemorrhagic ovarian cysts, which resolve, and malignancies, which progress.

Teaching Point

Teratomas

Another common complex mass arising from the ovary is the cystic teratoma or dermoid cyst. These lesions represent 96% of germ-cell tumors and 15% of all ovarian tumors (12). The vast majority of teratomas are mature and benign, with 99% demonstrating a cystic component. Teratomas are lined with squamous epithelium and contain elements from all three germ layers. They are bilateral in 15%–20% of cases, and they are associated with torsion in more than 15% of cases (13).

The US appearance is varied because of the presence of hyperechoic fat, teeth, and hair, as well as fluid in various amounts (Fig 8). Both predominantly cystic and predominantly solid masses have been described with approximately equal frequency. Echogenic shadowing mural nodules (Rokitansky nodules or dermoid plugs), which often contain hair or calcification, may be observed at US and are diagnostically specific (14). Complete posterior shadowing aids in the differentiation of mural nodules in teratomas from dependent thrombi in hemorrhagic cysts or endometriomas, which generally allow some posterior through-transmission (15).

On CT images, regions with fat attenuation are observed in more than 90% of cases. Mural nodules also are commonly seen on images that show the cyst wall in cross section, and they rarely enhance. Calcifications or teeth most often are found within mural nodules, but they also may be seen in cystic septa or walls. When cystic teratomas produce ovarian torsion, the resultant congestion and edema are manifested in thickening of the cyst wall, free pelvic fluid, or both (16).

Teaching Point

Cystadenomas

Serous and mucinous subtypes of cystadenoma represent the most common ovarian tumors. The majority of mucinous tumors occur in postmenopausal women and therefore are unlikely to be confused with the other acute pathologic entities described in this article.

When a cystadenoma is present, both US and CT depict a complex cystic adnexal mass with internal attenuation that varies with the proteinaceous content of the lesion. Like any adnexal mass, a cystadenoma predisposes the ovary to torsion; however, because the lesion grows slowly, its first manifestation is often chronic pelvic pain or an abdominal mass.

Torsion

Adnexal torsion occurs when the ovary, with the surrounding tissues, becomes twisted on its vascular pedicle. Torsion generally occurs in

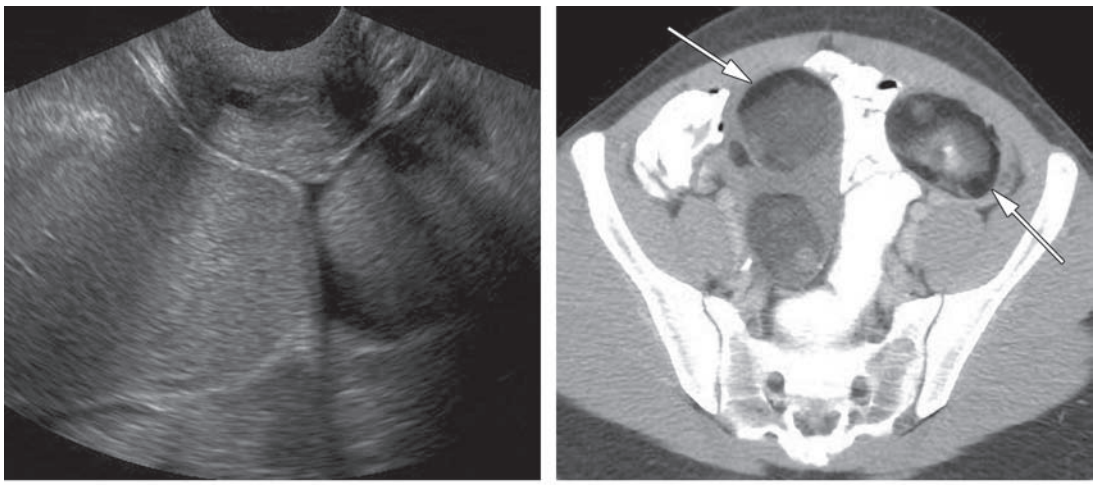

a. b.

Figure 8. Bilateral teratomas. **(a)** Transverse transvaginal US image shows well-delineated, largely isoechoic adnexal masses in close proximity at the midline. **(b)** Axial contrast-enhanced CT image demonstrates attenuation similar to that of fat within the bilateral masses (arrows), a finding diagnostic for teratoma. The diagnosis was confirmed at pathologic analysis.

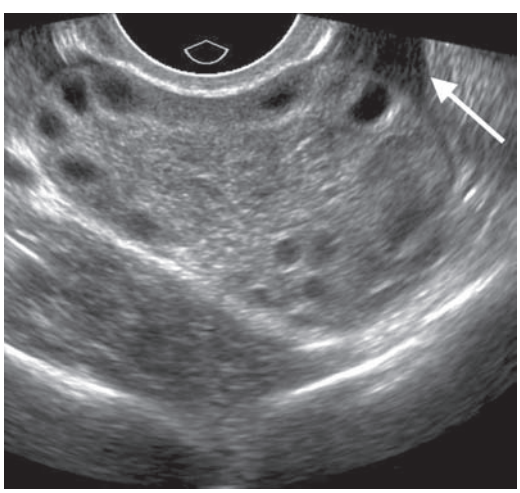

Figure 9. Adnexal torsion. Longitudinal transvaginal US image shows an enlarged ovary (maximal diameter, >5 cm) with prominent peripheral nonovulatory follicles and a small amount of free fluid (arrow) around the inferior margin.

the setting of a benign adnexal mass. However, torsion also may occur in normal ovaries, most commonly in prepubertal girls (17). Risk factors for torsion include pregnancy, primarily at 8–16 weeks of gestation, because of rapid changes in uterine size and morphology (18). Pelvic pain may be intermittent or may resolve in the presence of partial or intermittent torsion. The prompt diagnosis of torsion is critical to allow conservative ovary-sparing surgical intervention in young women.

The US appearance of torsion depends on its chronicity and severity; both complex cystic and solid masses have been described. As the vascular pedicle twists, the low-pressure conduits of the venous and lymphatic system become occluded. US findings that result from this occlusion of outflow include engorgement of the ovary, with central hyperechogenicity indicative of edema and with enlarged (up to 25 mm in diameter) nonovulatory follicles at the periphery (Fig 9). Ischemia contributes to edematous ovarian enlargement (19). Alternatively, US images may depict the cyst (or, less commonly, the mass) that predisposed the ovary to torsion. As torsion progresses, hemorrhagic infarction occurs, and corresponding hypoechoic regions are observed on US images. Free fluid also is commonly detected, but this finding is nonspecific.

Ovarian viability in the presence of torsion is difficult to determine. Since the ovary receives a dual arterial supply (from the aorta via the ovarian artery and from the adnexal, or ovarian, branch of the uterine artery), high-grade torsion is necessary to produce inflow occlusion. Color Doppler images that show an absence of arterial waveforms or high resistance to arterial flow with absent venous flow are highly suggestive of ovarian torsion, particularly when those findings are accompanied by ovarian enlargement. However, the converse does not hold true (ie, normal arterial waveforms do not rule out torsion). In a series of girls younger than 16 years, arterial flow was demonstrated in 40% of ovaries with proved torsion at laparoscopy (17). The absence

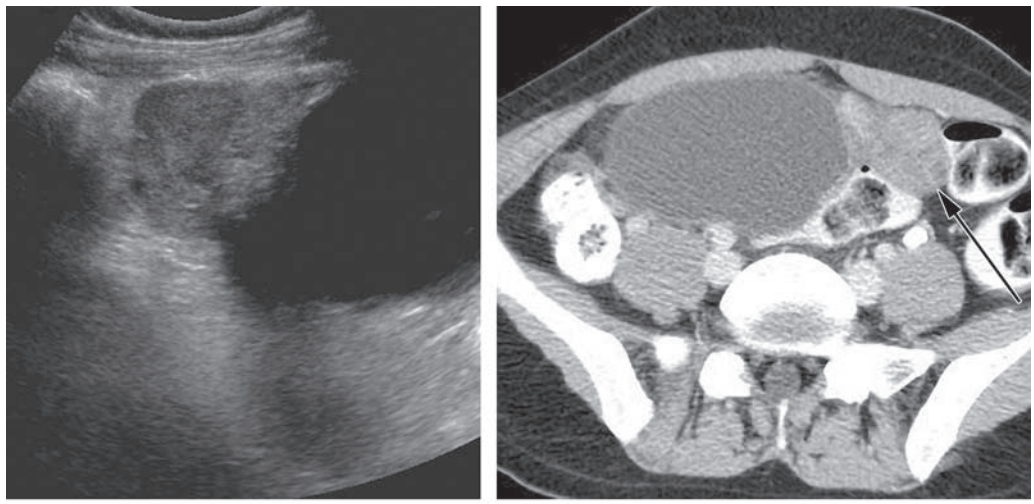

a. b.

Figure 10. Adnexal torsion. **(a)** Longitudinal transabdominal US image of the left adnexa shows a heterogeneous mass intimately associated with a large cystic mass. **(b)** Axial contrast-enhanced CT image depicts a heterogeneous left ovary (arrow) with a high-attenuation cyst that extends toward the right. At surgery, torsion induced by a benign hemorrhagic cyst of the left ovary was confirmed.

of arterial waveforms should be interpreted with consideration of the clinical manifestations and technical factors (eg, body habitus and distance of the ovary from the transducer).

Gray-scale US may directly depict the twisted vascular pedicle. As the transducer scans longitudinally along the vascular pedicle, real-time US reveals swirling of the vasculature. This so-called whirlpool sign is reported to be specific for adnexal torsion. In addition, color Doppler evaluation of the pedicle in the presence of torsion is thought to allow determination of ovarian viability (20). However, the reliability of such an evaluation is limited by the operator's skill, and, to our knowledge, there is no US sign that is widely acknowledged to be indicative of ovarian viability.

Teaching Point

At CT, the finding of an adnexal mass or enlarged ovary with a diameter of more than 5 cm may be suggestive of torsion. Smooth wall thickening to more than 3 mm in cystic adnexal masses also has been reported in the presence of torsion (21). Because of the thickened wall, the fallopian tube often has the appearance of a targetlike mass between the adnexa and uterus (Fig 10). Additional findings may include ascites and uterine deviation toward the affected side, which are present in more than 40% of cases (22). Lack of contrast enhancement, or hematoma due to hemorrhagic infarction, also may be depicted. However, the overall accuracy of CT is inferior to that of US in the preoperative diagnosis of adnexal torsion (23).

Nonovarian Adnexa

Paraovarian Cysts

Although paraovarian cysts are not of ovarian origin, they are categorized with other simple cysts that may cause pain due to rupture or torsion. Paraovarian cysts, which represent 10%–20% of all adnexal masses, arise from the pelvic mesothelium and paramesonephric tissue, although there are rare reports of paraovarian cysts with mesonephric (Wolffian) duct origin. The US and CT appearance of these cysts is similar to that of simple cysts found in other anatomic sites: well defined, unilocular, and containing homogeneously anechoic fluid (24). A diagnosis of paraovarian cyst is favored when the ovary is depicted as separate from the cyst; however, clear depiction of its separateness is often prevented by adnexal distortion (Fig 11). Large paraovarian cysts have been described in locations superior to the bladder, possibly having migrated there during their enlargement (25). Because paraovarian cysts are not hormonally responsive, their imaging appearance does not change over time. Stability at follow-up examinations during different

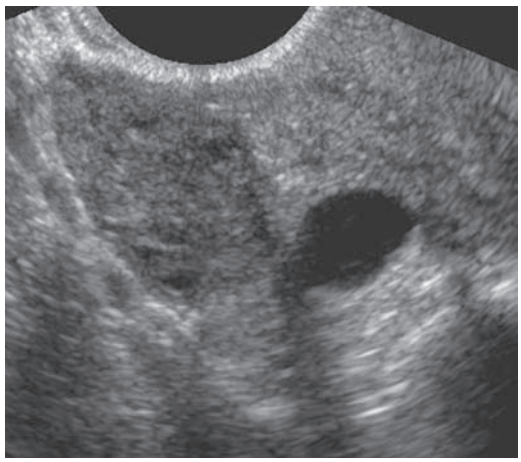

Figure 11. Paraovarian cyst. Transverse transvaginal US image of the adnexa shows an anechoic cyst with posterior through-transmission. The cyst is distinctly separate from the adjacent ovary.

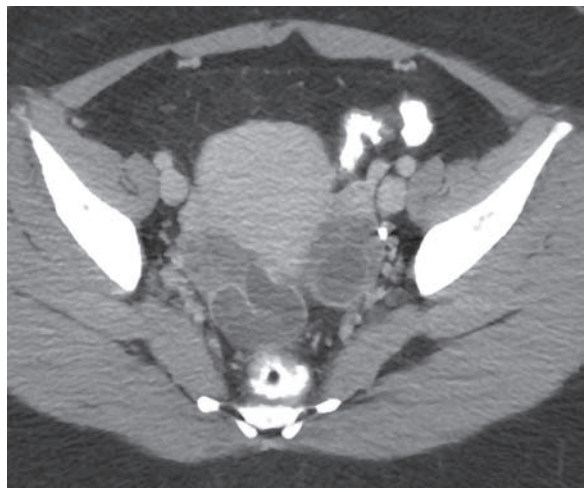

Figure 13. Hydrosalpinx. Axial contrast-enhanced CT image shows simple folded fluid-attenuation tubular structures in the bilateral adnexa with no adjacent inflammatory stranding or free fluid.

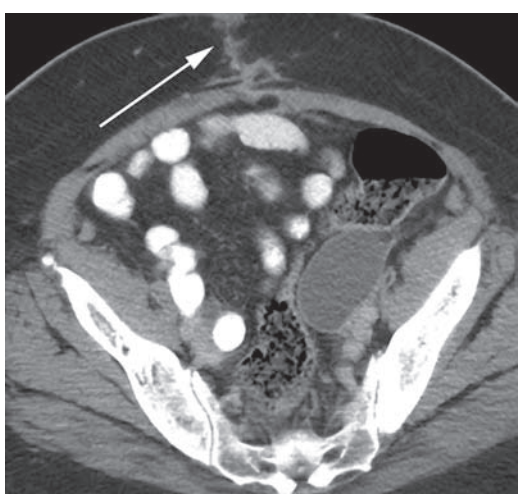

Figure 12. Peritoneal inclusion cyst. Axial contrast-enhanced CT image demonstrates a round, simple fluid collection in the left lower abdominal quadrant, immediately anterior to the external iliac vasculature, near a midline ventral incision site (arrow). The left ovary in this case is not separate from the cyst.

phases of the menstrual cycle, in particular, is suggestive of the diagnosis.

Peritoneal Inclusion Cysts

Pelvic adhesions that surround the ovary and create complex cystic masses must be differentiated from paraovarian cysts and hydrosalpinx. Previous surgery and pelvic inflammatory disease commonly result in a predisposition to the formation of such adhesions. US depicts a normal-appearing ovary that is surrounded by loculated fluid, in a pattern resembling a spider web (26). Diagnosis at CT may be more difficult. The fluid collections are often irregular, conforming to the borders of adjacent organs or the peritoneal wall. The wall of the collection itself is generally thicker than that of a paraovarian cyst (27) (Fig 12).

Hydrosalpinx

The fallopian tubes shuttle the ovum to the uterus for implantation. Typically 1–4 mm in diameter (28), the fallopian tubes are not regularly seen on US or CT images. At US, the depiction of normal fallopian tubes is possible only when they are outlined by ascites. Direct depiction otherwise is a marker of a pathologic process. When adhesions obstruct the fimbriated end of the fallopian tube, hydrosalpinx results because of the accumulation of intraluminal secretions.

US depicts the fallopian tube as a fusiform tubular structure extending between the uterus and adnexa. Tapering of the proximal fallopian tube as it enters the uterus is a useful sign for anatomic localization. The internal fluid is anechoic, and dynamic imaging reveals multiple folds in the tube (28) (Fig 13). Real-time US has the added advantage of documenting the absence

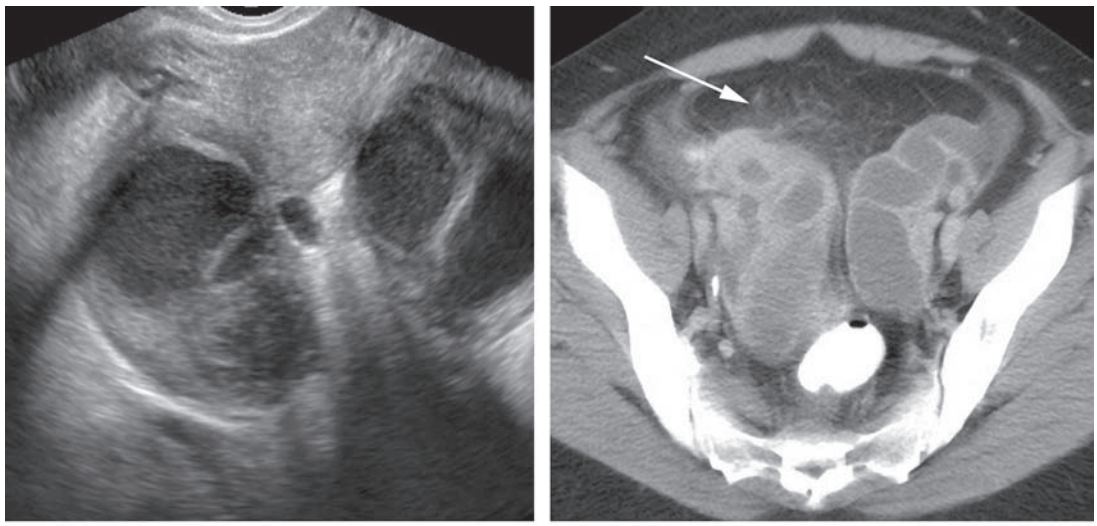

a. b.

Figure 14. Pelvic inflammatory disease with a tuboovarian abscess. **(a)** Transverse transvaginal US image of the pelvis reveals bilateral dilated folding tubular structures with thickened walls, internal echogenic fluid, and debris. **(b)** Axial contrast-enhanced CT image shows dilated tubular structures with thick enhancing walls. Inflammatory stranding of the surrounding fat is most demonstrable on the right (arrow). The presence of a tuboovarian abscess was confirmed at surgery.

of peristalsis within the fallopian tube, a finding that helps differentiate hydrosalpinx from a fluid-filled loop of small bowel. Isolated torsion of the fallopian tubes without an adnexal abnormality is possible but rare, with an estimated incidence of one in 1.5 million women (29). The occurrence of isolated torsion after tubal ligation is signaled by fusiform tubal dilatation and surrounding pelvic inflammation. Hydrosalpinx has a similar appearance at CT, which generally shows paired tubular juxtauterine structures filled with simple fluid.

Ectopic Pregnancy

Ectopic pregnancy is always a consideration in women of reproductive age with acute pelvic pain and with a positive β-hCG level. Imaging features of ectopic pregnancy are described in another article in this issue (30) and therefore are not discussed here.

Pelvic Inflammatory Disease

Pelvic inflammatory disease refers to a gamut of infectious conditions of the upper reproductive tract, including endometritis, salpingitis, and tuboovarian abscess. The source of disease is typically an ascending lower tract infection, although hematogenous spread and direct extension of an infection (eg, from an adjacent abscess) also are possible. *Neisseria gonorrhoeae* or *Chlamydia trachomatis* is believed to be the offending agent in two-thirds of cases, but polymicrobial infection also has been reported (31). As many as 24% of visits to the emergency department for gynecologic pain are attributable to pelvic inflammatory disease. Presentation with a report of dull and aching pain usually occurs 7–10 days after menstruation (1).

Early in the course of such an infection, US and CT findings may be normal. As the infection progresses, US demonstrates a loss of normal tissue planes and an ill-defined uterus. Uterine enlargement may be present and is most noticeable at transabdominal US. Thickening of the endometrium may be present but is nonspecific. Because fluid within the endometrial canal may mimic a gestational sac, this finding should be correlated with the β-hCG level.

Salpingitis may progress to hydrosalpinx or pyosalpinx if left untreated. In pyosalpinx, US images show complex fluid with echogenic debris distending the fallopian tubes. Other imaging clues include folding of the tubular structure, tapering of the ends, and short linear echogenic foci projecting into the lumen (32). At later stages, tuboovarian abscesses may form. This continuum involves the production of increasing amounts of inflammatory exudates, pus, and

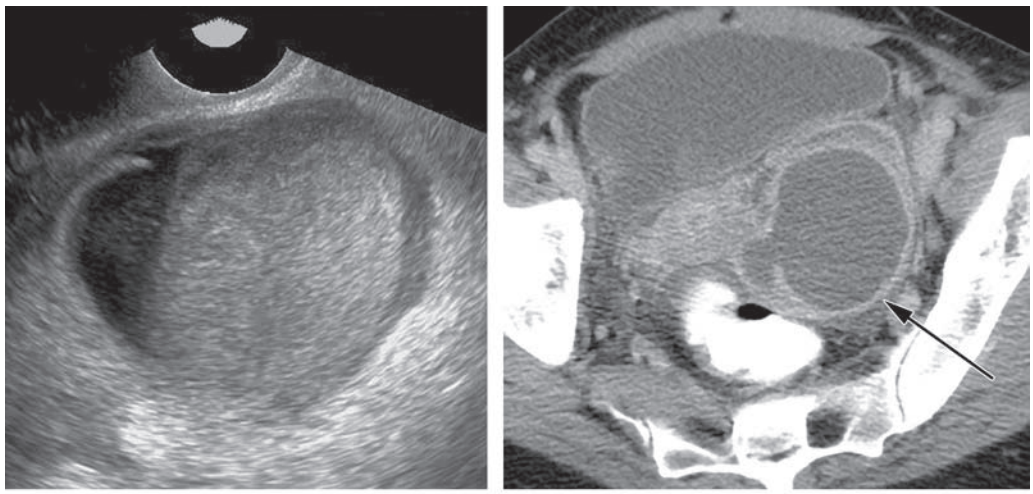

a. b.

Figure 15. Pelvic abscess. **(a)** Transverse transvaginal US image of the left adnexa demonstrates a well-defined mass with thick walls and an internal fluid-debris level. **(b)** Axial contrast-enhanced CT image helps confirm the presence of a left adnexal tuboovarian abscess (arrow) with thick enhancing walls and complex internal fluid. The abscess resolved with conservative therapy.

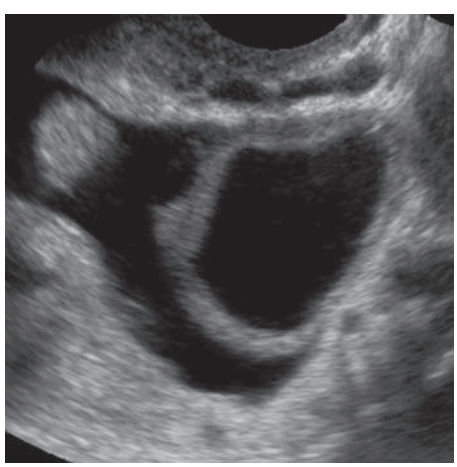

Figure 16. Ruptured ovarian cyst. Transverse transvaginal US image of the right adnexa shows a thick-walled ovarian cyst (corpus luteum) with surrounding anechoic free fluid, a finding indicative of rupture.

blood, which are depicted as echogenic debris within the fallopian tubes (Fig 14a). Involvement is often bilateral. Movement of the fallopian tubes under gentle pressure from the US transducer may be minimal because of adhesions.

CT is employed when a nongynecologic pathologic entity is suspected to be the cause of low abdominal pain or when a global view of a gynecologic disease process is needed. Stranding of the parapelvic fat is common but nonspecific. The uterosacral ligaments may appear thickened. When a tuboovarian abscess is present, CT images show complex fluid-attenuation collections with thickened and irregularly enhancing walls (Fig 14b). Anterior displacement of the broad ligament because of the posterior position of the mesovarium may allow differentiation of a tuboovarian abscess from a pelvic abscess of other origin (33). Unlike tuboovarian abscesses, which result from an ascending pelvic infection, general pelvic abscesses result from an adjacent infection in the appendix, colon, or (uncommonly) bladder. These abscesses may have a thicker wall and may be located at a distance from the adnexa (Fig 15).

Teaching Point

Free Pelvic Fluid

Free intraperitoneal fluid is demonstrable at US and CT. A small simple fluid collection (3–5 mL) that is anechoic at US and has attenuation of less than 20 HU at CT is often physiologic. A collection of more than 10 mL should arouse concern about the possibility of a pathologic process (2). Although free intraperitoneal fluid usually is found in the most dependent region of the pelvis, the rectouterine pouch of Douglas, fluid also may be depicted immediately adjacent to a ruptured ovarian cyst (Fig 16). When the presence of a pathologic fluid collection is suspected but not

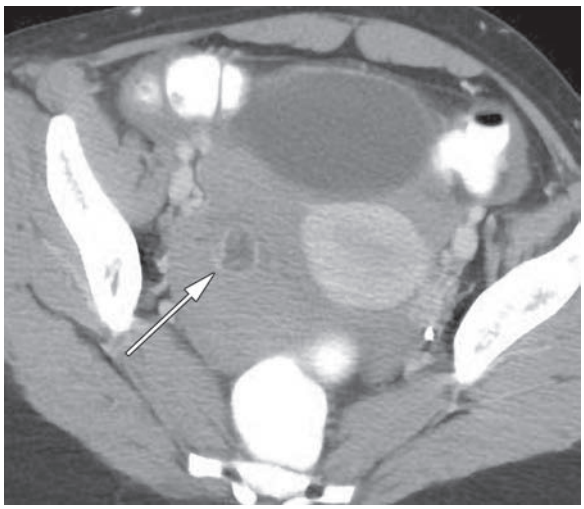

Figure 17. Ruptured corpus luteum with hemoperitoneum. Axial contrast-enhanced CT image depicts a corpus luteum with an enhancing wall (arrow) in the right ovary and a significant amount of high-attenuation pelvic fluid surrounding the enhancing uterus, findings indicative of corpus luteum hemorrhage and rupture.

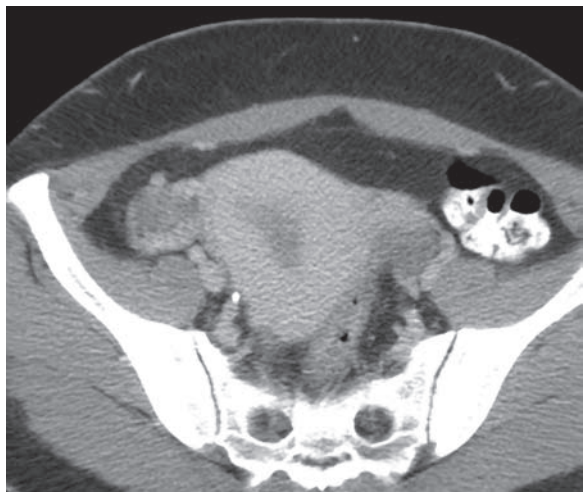

Figure 18. Normal uterus. Axial contrast-enhanced CT image shows the normal differential enhancement of the myometrium and endometrium. The endometrium has relatively lower attenuation and shows less enhancement, an appearance that might lead to its being mistaken for fluid.

immediately demonstrated at US, a search at the superior junction of the bladder and uterus may prove fruitful (34).

Complex fluid collections contain echogenic debris at US and show increased attenuation at CT. Their differentiation from simple fluid collections may help guide patient management. Hemoperitoneum is a positive predictive factor for ectopic pregnancy in the setting of a positive β-hCG level (35). Similarly, hemoperitoneum in the presence of hemodynamic instability should prompt laparotomy, regardless of additional findings (Fig 17).

Uterus

Uterine abnormalities that may cause pelvic pain may be broadly divided into pregnancy- and nonpregnancy-associated conditions, with β-hCG levels guiding clinical differentiation between the two. Uterine detail is most readily assessed with endovaginal US. Endometrial thickness varies with the stage of the menstrual cycle, measuring up to 18 mm during the secretory phase. Endometrial thickness greater than 4–5 mm is abnormal in postmenopausal patients. The endometrium has attenuation lower than the adjacent myometrium on CT images but higher than that of fluid (Fig 18). Although a finding of endometrial fluid in the nongravid uterus is nonspecific, it has been described in association with cystic teratomas and ruptured corpus luteum cysts (36).

Figure 19. Pedunculated fibroid. Longitudinal transvaginal US image depicts a heterogeneous, slightly hypoechoic mass (arrow) that is clearly attached to the anterior margin of the uterine fundus.

Fibroids

Benign smooth-muscle tumors (leiomyomas and fibroids) are the most common tumors of the uterus; they are found in more than one-fifth of women over the age of 30 years (9). These estrogen-dependent tumors are found, in order of decreasing frequency, in an intramural, subse-

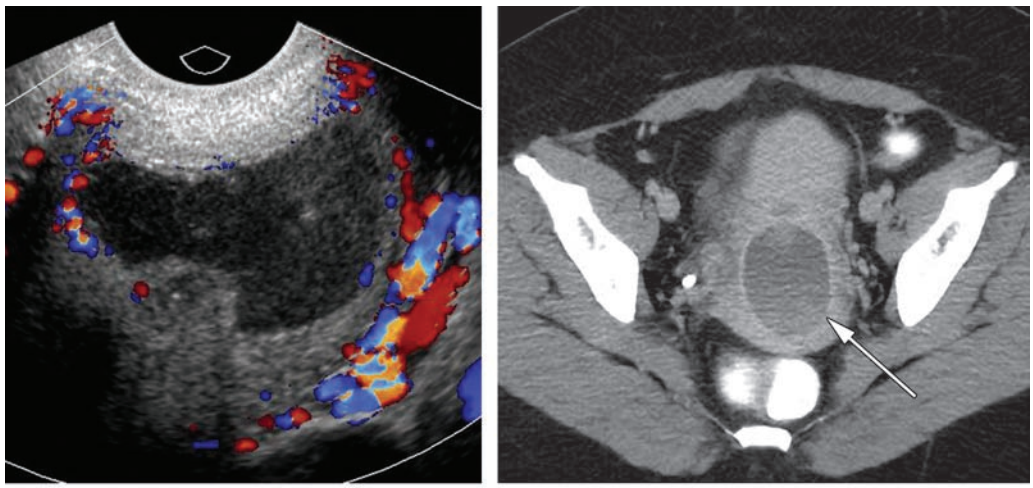

a. b.

Figure 20. Degenerating fibroid. **(a)** Longitudinal transvaginal color Doppler US image of the inferior part of the uterus demonstrates a complex cystic mass with internal echogenicity and no internal vascularity. **(b)** Axial contrast-enhanced CT image shows an isoattenuating uterine mass with a well-defined complex cystic center (arrow) containing fluid and debris layering, a feature indicative of hemorrhagic degeneration.

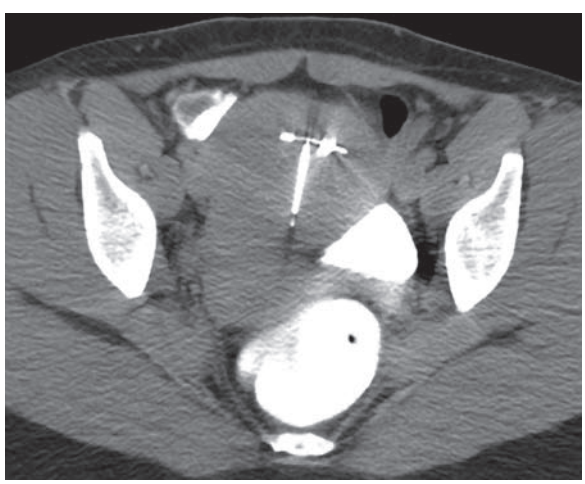

Figure 21. Intrauterine contraceptive device. Axial CT image shows a T-shaped device in the appropriate position.

rosal, or submucosal location. Multiple forms of degeneration (eg, hemorrhagic, cystic, myxoid) occur when the fibroid outgrows its blood supply, causing pelvic pain in as many as 30% of cases. Alternatively, presentation may be due to vaginal bleeding. Sarcomatous degeneration to leiomyosarcoma is rare, occurring in less than 0.1% of cases (5). Benign degeneration, hemorrhage, or compression of adjacent structures may precipitate pelvic pain. Pregnancy may cause a predisposition to hemorrhagic, or red, degeneration of a uterine fibroid. Such an occurrence is most likely during the period of greatest increase in myometrial volume, generally before 10 weeks of gestation (37). Pedunculated fibroids are predisposed to torsion (38) (Fig 19).

US shows a solid uterine mass, typically with minimal echotexture (Fig 20a), although heterogeneity may result from necrotic degeneration. Calcifications within the fibroid, which are more common in older patients, appear as hyperechoic foci with posterior shadowing, but that finding is of little clinical relevance. CT is helpful for confirming US findings of a solid soft-tissue uterine mass. The uterus may be enlarged. A lobulated uterine contour has been reported in the presence of fibroids that extend beyond the mucosal or serosal layer. A central region of low attenuation within a fibroid is suggestive of internal degeneration, and heterogeneous contrast enhancement may be present (Fig 20b). Pedunculated subserosal fibroids have been described as juxtauterine masses with peripheral enhancement and necrotic centers at CT (9,38).

Intrauterine Contraceptive Devices

Intrauterine device placement is commonly performed for the purpose of contraception. The US and CT appearances vary according to the type of device, but a T-shaped device is the most commonly seen within the uterus (Fig 21). The

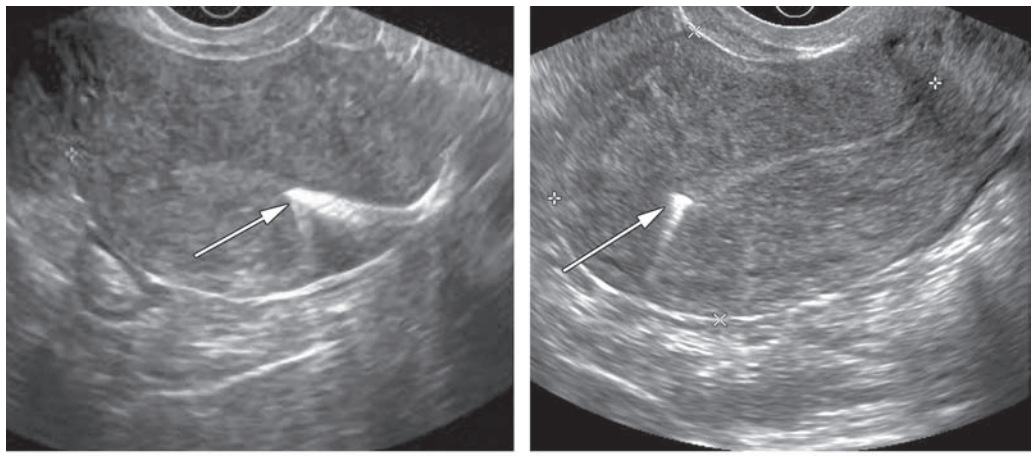

a. b.

Figure 22. Migration of a contraceptive device. Longitudinal **(a)** and transverse **(b)** transvaginal US images of the uterus show a linear echogenic fallopian tube occlusion device (arrow) that has migrated into the left posterior region of the myometrium.

device appears well defined, hyperechoic at US, and hyperattenuating at CT. Rarely (in approximately 0.1% of cases), perforation into or through the myometrium may occur as a complication of intrauterine device placement (39). When perforation occurs, hemorrhage and free pelvic fluid are possible, with associated pelvic pain. The finding of an intrauterine device within the myometrium is highly suggestive of perforation. A device also may migrate by tracking into a surgical scar. Linear coils designed to occlude the fallopian tubes may migrate into the endometrial canal or enter the myometrium by perforation (Fig 22).

Summary

Multiple entities, including normal physiologic changes, may cause acute pelvic pain in premenopausal patients. Correlation of the individual clinical history with imaging features (especially the anatomic location and morphologic characteristics) is beneficial for narrowing the diagnostic possibilities. Knowledge of the common US and CT appearances of various normal and abnormal gynecologic conditions allows their accurate diagnosis and expeditious management.

References

1. Samraj GP, Curry RW Jr. Acute pelvic pain: evaluation and management. Compr Ther 2004;30:173–184.
2. Jones HW. Pelvic pain: overview. In: Fleischer AC, Javitt MC, Jeffrey RB, Jones HW, eds. Clinical gynecologic imaging. Philadelphia, Pa: Lippincott-Raven, 1997; 245–248.
3. Dodson MG. The ovary. In: Dodson MG, ed. Transvaginal ultrasound. 2nd ed. New York, NY: Churchill Livingstone, 1995; 105–132.
4. Kalish GM, Patel MD, Gunn ML, Dubinsky TJ. Computed tomography and magnetic resonance features of gynecologic abnormalities in women presenting with acute or chronic abdominal pain. Ultrasound Q 2007;23:167–175.
5. Di Salvo DN. Sonographic imaging of maternal complications of pregnancy. J Ultrasound Med 2003;22:69–89.
6. Jain KA. Sonographic spectrum of hemorrhagic ovarian cysts. J Ultrasound Med 2002;21:879–886.
7. Borders RJ, Breiman RS, Yeh BM, Qayyum A, Coakley FV. Computed tomography of corpus luteal cysts. J Comput Assist Tomogr 2004;28:340–342.
8. Patel MD, Feldstein VA, Filly RA. The likelihood ratio of sonographic findings for the diagnosis of hemorrhagic ovarian cysts. J Ultrasound Med 2005; 24:607–614.

9. Bennett GL, Slywotzky CM, Giovanniello G. Gynecologic causes of acute pelvic pain: spectrum of CT findings. RadioGraphics 2002;22:785–801.
10. Chang WC, Meux MD, Yeh BM, et al. CT and MRI of adnexal masses in patients with primary nonovarian malignancy. AJR Am J Roentgenol 2006;186:1039–1045.
11. Friedman H, Vogelzang RL, Mendelson EB, Neiman HL, Cohen M. Endometriosis detection by US with laparoscopic correlation. Radiology 1985; 157:217–220.
12. Kurjak A, Kupesic S, Babic MM, Goldenburg M, Illijas M, Kosuta D. Preoperative evaluation of cystic teratoma: what does color Doppler add? J Clin Ultrasound 1997;25:309–316.
13. Talerman A. Germ cell tumors of the ovary. In: Altchek A, Deligdisch L, Kase NG, eds. Diagnosis and management of ovarian disorders. 2nd ed. Amsterdam, the Netherlands: Academic Press, 2003; 95–110.
14. Buy JN, Ghossain MA, Moss AA, et al. Cystic teratoma of the ovary: CT detection. Radiology 1989; 171:697–701.
15. Patel MD, Feldstein VA, Lipson SD, Chen DC, Filly RA. Cystic teratomas of the ovary: diagnostic value of sonography. AJR Am J Roentgenol 1998; 171:1061–1065.
16. Quinn SF, Erickson S, Black WC. Cystic ovarian teratomas: the sonographic appearance of the dermoid plug. Radiology 1985;155:477–478.
17. Stark JE, Siegel MJ. Ovarian torsion in prepubertal and pubertal girls: sonographic findings. AJR Am J Roentgenol 1994;163:1479–1482.
18. Pena JE, Ufberg D, Cooney N, Denis AL. Usefulness of Doppler sonography in the diagnosis of ovarian torsion. Fertil Steril 2000;73:1047–1050.
19. Graif M, Shalev J, Strauss S, Engelberg S, Mashiach S, Itzchak Y. Torsion of the ovary: sonographic features. AJR Am J Roentgenol 1984;143:1331–1334.
20. Vijayaraghavan SB. Sonographic whirlpool sign in ovarian torsion. J Ultrasound Med 2004;23:1643–1649.
21. Ghossain MA, Buy JN, Bazot M, et al. CT in adnexal torsion with emphasis on tubal findings: correlation with US. J Comput Assist Tomogr 1994;18: 619–625.
22. Hiller N, Appelbaum L, Simanovsky N, Lev-Sagi A, Aharoni D, Tamar S. CT features of adnexal torsion. AJR Am J Roentgenol 2007;189:124–129.
23. Chiou SY, Lev-Toaff AS, Masuda E, Feld RI, Bergin D. Adnexal torsion: new clinical and imaging observations by sonography, computed tomography, and magnetic resonance imaging. J Ultrasound Med 2007;26:1289–1301.
24. Alpern MB, Sandler MA, Madrazo BL. Sonographic features of parovarian cysts and their complications. AJR Am J Roentgenol 1984;143:157–160.
25. Athey PA, Cooper NB. Sonographic features of parovarian cysts. AJR Am J Roentgenol 1985;144: 83–86.
26. Kim JS, Lee HJ, Woo SK, Lee TS. Peritoneal inclusion cysts and their relationship to the ovaries: evaluation with sonography. Radiology 1997;204:481–484.
27. Kurachi H, Murakami T, Nakamura H, et al. Imaging of peritoneal pseudocysts: value of MR imaging compared with sonography and CT. AJR Am J Roentgenol 1993;161:589–591.
28. Orazi C, Inserra A, Lucchetti MC, Schingo PM. Isolated tubal torsion: a rare cause of pelvic pain at menarche. Pediatr Radiol 2006;36:1316–1318.
29. Anderson TL. Pelvic inflammatory disease: overview. In: Fleischer AC, Javitt MC, Jeffrey RB, Jones HW, eds. Clinical gynecologic imaging. Philadelphia, Pa: Lippincott-Raven, 1997; 231–235.
30. Lin EP, Bhatt S, Dogra VS. Diagnostic clues to ectopic pregnancy. RadioGraphics 2008;28:1661–1671.
31. Tessler FN, Perrella RR, Fleischer AC, Grant EG. Endovaginal sonographic diagnosis of dilated fallopian tubes. AJR Am J Roentgenol 1989;153:523–525.
32. Sam JW, Jacobs JE, Birnbaum BA. Spectrum of CT findings in acute pyogenic pelvic inflammatory disease. RadioGraphics 2002;22:1327–1334.
33. Wilbur AC, Aizenstein RI, Napp TE. CT findings in tuboovarian abscess. AJR Am J Roentgenol 1992; 158:575–579.
34. Nyberg DA, Laing FC, Jeffrey RB. Sonographic detection of subtle pelvic collections. AJR Am J Roentgenol 1984;143:261–263.
35. Jeffrey RB, Laing FC. Echogenic clot: a useful sign of pelvic hemoperitoneum. Radiology 1982;145: 139–141.
36. Laing FC, Filly RA, Marks WM, Brown TW. Ultrasonic demonstration of endometrial fluid collections unassociated with pregnancy. Radiology 1980;137:471–474.
37. Eyvazzadeh AD, Levine D. Imaging of pelvic pain in the first trimester of pregnancy. Radiol Clin North Am 2006;44:863–877.
38. Roy C, Bierry G, El Ghali S, Buy X, Rossini A. Acute torsion of uterine leiomyoma: CT features. Abdom Imaging 2005;30:120–123.
39. Peri N, Graham D, Levine D. Imaging of intrauterine contraceptive devices. J Ultrasound Med 2007;26:1389–1401.

This article meets the criteria for 1.0 AMA PRA Category 1 Credit™. To obtain credit, see www.rsna.org/education/rg_cme.html.

US and CT Evaluation of Acute Pelvic Pain of Gynecologic Origin in Nonpregnant Premenopausal Patients

Andrew W. Potter, MD, and Chitra A. Chandrasekhar, MBBS

RadioGraphics 2008; 28:1645–1659 • **Published online** 10.1148/rg.286085504 • **Content Codes:** CT ER OB US

Page 1649
The typical appearance is that of a complex mass with internal echoes and some degree of posterior through-transmission. Although fresh blood may be anechoic initially, a hemorrhagic cyst is defined by low-level echogenicity in a fine, lacelike, reticular pattern for the first 24 hours, and this pattern is diagnostically specific.

Page 1650
Both US and CT findings have low specificity for the diagnosis of endometriomas. Follow-up imaging is useful for differentiating endometriomas from pathologic entities such as hemorrhagic ovarian cysts, which resolve, and malignancies, which progress.

Page 1650
On CT images, regions with fat attenuation are observed in more than 90% of cases. Mural nodules also are commonly seen on images that show the cyst wall in cross section, and they rarely enhance.

Page 1652
At CT, the finding of an adnexal mass or enlarged ovary with a diameter of more than 5 cm may be suggestive of torsion. Smooth wall thickening to more than 3 mm in cystic adnexal masses also has been reported in the presence of torsion.

Page 1655
When a tuboovarian abscess is present, CT images show complex fluid-attenuation collections with thickened and irregularly enhancing walls. Anterior displacement of the broad ligament because of the posterior position of the mesovarium may allow differentiation of a tuboovarian abscess from a pelvic abscess of other origin.

RadioGraphics 2008

This is your reprint order form or pro forma invoice

(Please keep a copy of this document for your records.)

Reprint order forms and purchase orders or prepayments must be received 72 hours after receipt of form either by mail or by fax at 410-820-9765. It is the policy of Cadmus Reprints to issue one invoice per order. **Please print clearly**.

Author Name _____
Title of Article _____
Issue of Journal_____ Reprint # _____ Publication Date _____
Number of Pages_____ KB # _____ Symbol RadioGraphics
Color in Article? Yes / No (Please Circle)

Please include the journal name and reprint number or manuscript number on your purchase order or other correspondence.

Order and Shipping Information

Reprint Costs **(Please see page 2 of 2 for reprint costs/fees.)**

_____ Number of reprints ordered $_____
_____ Number of color reprints ordered $_____
_____ Number of covers ordered $_____
Subtotal $_____
Taxes $_____

(*Add appropriate sales tax for Virginia, Maryland, Pennsylvania, and the District of Columbia or Canadian GST to the reprints if your order is to be shipped to these locations*.)

First address included, add $32 for each additional shipping address $_____

TOTAL $_____

Shipping Address **(cannot ship to a P.O. Box) Please Print Clearly**

Name _____
Institution _____
Street _____
City _____ State _____ Zip _____
Country _____
Quantity_____ Fax _____
Phone: Day _____ Evening _____
E-mail Address _____

Additional Shipping Address* **(cannot ship to a P.O. Box)**

Name _____
Institution _____
Street _____
City _____ State _____ Zip _____
Country _____
Quantity _____ Fax _____
Phone: Day _____ Evening _____
E-mail Address _____

** Add $32 for each additional shipping address*

Payment and Credit Card Details

Enclosed: Personal Check _____
Credit Card Payment Details _____
Checks must be paid in U.S. dollars and drawn on a U.S. Bank.

Credit Card: __ VISA __ Am. Exp. __ MasterCard
Card Number _____
Expiration Date_____
Signature: _____

Please send your order form and prepayment made payable to:

Cadmus Reprints
P.O. Box 751903
Charlotte, NC 28275-1903

Note: Do not send express packages to this location, PO Box.
FEIN #:541274108

Invoice or Credit Card Information

Invoice Address Please Print Clearly
Please complete Invoice address as it appears on credit card statement

Name _____
Institution _____
Department _____
Street _____
City _____ State _____ Zip _____
Country _____
Phone _____ Fax _____
E-mail Address _____

Cadmus will process credit cards and *Cadmus Journal Services* will appear on the credit card statement.

If you don't mail your order form, you may fax it to 410-820-9765 with your credit card information.

Signature _____ Date _____

Signature is required. By signing this form, the author agrees to accept the responsibility for the payment of reprints and/or all charges described in this document.

RB-9/26/07

RadioGraphics 2008

Black and White Reprint Prices

Domestic (USA only)						
# of Pages	50	100	200	300	400	500
1-4	$221	$233	$268	$285	$303	$323
5-8	$355	$382	$432	$466	$510	$544
9-12	$466	$513	$595	$652	$714	$775
13-16	$576	$640	$749	$830	$912	$995
17-20	$694	$775	$906	$1,017	$1,117	$1,220
21-24	$809	$906	$1,071	$1,200	$1,321	$1,471
25-28	$928	$1,041	$1,242	$1,390	$1,544	$1,688
29-32	$1,042	$1,178	$1,403	$1,568	$1,751	$1,924
Covers	$97	$118	$215	$323	$442	$555

International (includes Canada and Mexico)						
# of Pages	50	100	200	300	400	500
1-4	$272	$283	$340	$397	$446	$506
5-8	$428	$455	$576	$675	$784	$884
9-12	$580	$626	$805	$964	$1,115	$1,278
13-16	$724	$786	$1,023	$1,232	$1,445	$1,652
17-20	$878	$958	$1,246	$1,520	$1,774	$2,030
21-24	$1,022	$1,119	$1,474	$1,795	$2,108	$2,426
25-28	$1,176	$1,291	$1,700	$2,070	$2,450	$2,813
29-32	$1,316	$1,452	$1,936	$2,355	$2,784	$3,209
Covers	$156	$176	$335	$525	$716	$905

Minimum order is 50 copies. For orders larger than 500 copies, please consult Cadmus Reprints at 800-407-9190.

Reprint Cover

Cover prices are listed above. The cover will include the publication title, article title, and author name in black.

Shipping

Shipping costs are included in the reprint prices. Domestic orders are shipped via UPS Ground service. Foreign orders are shipped via a proof of delivery air service.

Multiple Shipments

Orders can be shipped to more than one location. Please be aware that it will cost $32 for each additional location.

Delivery

Your order will be shipped within 2 weeks of the journal print date. Allow extra time for delivery.

Color Reprint Prices

Domestic (USA only)						
# of Pages	50	100	200	300	400	500
1-4	$223	$239	$352	$473	$597	$719
5-8	$349	$401	$601	$849	$1,099	$1,349
9-12	$486	$517	$852	$1,232	$1,609	$1,992
13-16	$615	$651	$1,105	$1,609	$2,117	$2,624
17-20	$759	$787	$1,357	$1,997	$2,626	$3,260
21-24	$897	$924	$1,611	$2,376	$3,135	$3,905
25-28	$1,033	$1,071	$1,873	$2,757	$3,650	$4,536
29-32	$1,175	$1,208	$2,122	$3,138	$4,162	$5,180
Covers	$97	$118	$215	$323	$442	$555

International (includes Canada and Mexico))						
# of Pages	50	100	200	300	400	500
1-4	$278	$290	$424	$586	$741	$904
5-8	$429	$472	$746	$1,058	$1,374	$1,690
9-12	$604	$629	$1,061	$1,545	$2,011	$2,494
13-16	$766	$797	$1,378	$2,013	$2,647	$3,280
17-20	$945	$972	$1,698	$2,499	$3,282	$4,069
21-24	$1,110	$1,139	$2,015	$2,970	$3,921	$4,873
25-28	$1,290	$1,321	$2,333	$3,437	$4,556	$5,661
29-32	$1,455	$1,482	$2,652	$3,924	$5,193	$6,462
Covers	$156	$176	$335	$525	$716	$905

Tax Due

Residents of Virginia, Maryland, Pennsylvania, and the District of Columbia are required to add the appropriate sales tax to each reprint order. For orders shipped to Canada, please add 7% Canadian GST unless exemption is claimed.

Ordering

Reprint order forms and purchase order or prepayment is required to process your order. Please reference journal name and reprint number or manuscript number on any correspondence. You may use the reverse side of this form as a proforma invoice. Please return your order form and prepayment to:

Cadmus Reprints
P.O. Box 751903
Charlotte, NC 28275-1903

Note: Do not send express packages to this location, PO Box.
FEIN #:541274108

Please direct all inquiries to:

Rose A. Baynard
800-407-9190 (toll free number)
410-819-3966 (direct number)
410-820-9765 (FAX number)
baynardr@cadmus.com (e-mail)

Reprint Order Forms and purchase order or prepayments must be received 72 hours after receipt of form.